Hard Acid and Soft Base Stabilisation of Di- and Trimercury Cations in Benzene Solution – A Spectroscopic, X-ray Scattering, and Quantum Chemical Study

Stefan Ulvenlund,[a] Jan Rosdahl,[b] Andreas Fischer,[b] Peter Schwerdtfeger,[c] and Lars Kloo*[b]

Dedicated to Prof. Warren R. Roper on the occation of his 60th birthday

Keywords: Mercury cations / Subvalent compounds / Ab initio calculations / Liquid X-ray scattering

Hg_2Cl_2 dissolves in $GaCl_3$/benzene solution to yield Hg_2^{2+} and chlorogallate(III) ions, $Ga_nCl_{3n+1}^-$. In such solutions, Hg_2^{2+} can be reduced to Hg_3^{2+} by metallic mercury. Solubility measurements show that one mol of Hg is oxidised per mol of Hg_2^{2+}. The Hg_3^{2+} ion gives a strong band at 110 cm^{-1} in the Raman spectrum and Hg–Hg correlations at about 2.60 and 5.15 Å in the radial distribution function obtained by liquid X-ray scattering. – Hg_3^{2+} can also be synthesised in high yield by direct oxidation of metallic mercury by Ga^{III} in $GaCl_3$/benzene solution. In contrast, mercury is insoluble in neat liquid $GaCl_3$ and only sparingly soluble in $GaCl_3$/KCl melts. It therefore seems likely that the thermodynamic stabilisation of subvalent mercury species in benzene solution not only relies on the traditional acid stabilisation provided by the hard Lewis acid $GaCl_3$, but also on a "soft-base stabilisation" provided by interactions between the aromatic molecules and the cations. Evidence for such specific interactions between Hg_m^{2+} cations and C_6H_6 are observed in the Raman spectra: The totally symmetric C_6H_6 band at 991 cm^{-1} is found to split in the presence of Hg_m^{2+} ions and to give new peaks at 978 (m = 2) and 982 (m = 3) cm^{-1}. – In order to further elucidate the cluster–arene interactions, ab initio and density functional calculations were performed for the model compounds $Hg_m(C_6H_6)_2^{2+}$ and $Hg_mCl_2(C_6H_6)_2$, m = 2 and 3. The calculations show that both models represent coordinations modes which are feasible for Hg_m^{2+} ions. However, the calculated vibrational frequencies for the $Hg_m(C_6H_6)_2^{2+}$ models with η^1/*quasi*-η^3 coordination of the benzene molecules along the Hg–Hg vector are most consistent with the body of experimental and literature data. The counterions are thus suggested to occupy secondary coordination sites.

Introduction

Mercury displays a rich and unusual subvalent chemistry. In addition to the well-known dimer Hg_2^{2+}, previously reported metal−metal-bonded, subvalent mercury species include the linear cations Hg_3^{2+} and Hg_4^{2+}, which have been structurally characterised as salts of the weakly coordinating anions $AlCl_4^-$,[1] AsF_6^-,[2−4] $Ta_2F_{11}^-$,[5] and $[(MF_5)_2SO_4]^{2-}$ (M = Nb, Ta).[5] Mercury also forms infinite, one-dimensional chains in the non-stoichiometric compounds Hg_xTiS_2[6][7] and $Hg_{3-\delta}MF_6$ (M = As,[8−10] Sb,[11] Nb or Ta[12]), some of which transform into stoichiometric, layered compounds $Hg_3(MF_6)$ under appropriate conditions.[13] The fascinating physical properties of these anisotropic compounds have been investigated in considerable detail,[14−19] and are highlighted by the recent assignment of the well-known orange luminescence of calomel to Hg_3^{2+}, presumably formed by disproportionation of Hg_2Cl_2.[20]

As is the case with the vast majority of subvalent post-transition element species (apart from the anomalously stable Hg_2^{2+} cation), the traditional synthetic routes to subvalent mercury cations are based on molten-salt solutions, superacid media, or solutions of strongly oxidising fluorides in liquid SO_2. These highly Lewis-acidic solvent systems have been considered necessary in order to impede the disproportionation of the subvalent cations to higher, more acidic oxidation states and the parent metal.[21] However, triangular Hg_3^{4+} and $AgHg_2^{3+}$ species have recently been stabilised by diphosphanes in the direct reduction of divalent mercury in the presence of the phosphane ligand.[22−24] This route involves reaction media which are immensly more Lewis-basic than the traditional ones. In addition, it comprises *soft*, rather than hard, donors.

In recent publications we have described the syntheses of bismuth clusters and subvalent gallium species by a novel route employing solutions of $GaCl_3$ in organic (aromatic) solvents as reaction media.[25−28] The spectroscopic data for these systems suggest substantial interactions between subvalent metal species and aromatic donors. These donors have, of course, a pronounced soft character. Considering the recent success of stabilising subvalent mercury species in systems comprising other soft donors (i.e. diphosphanes), the $GaCl_3$/arene route is thus of great potential interest for

[a] Department of Explorative Pharmaceutics, Astra Draco AB, P. O. Box 34, S-22100 Lund, Sweden
[b] Inorganic Chemistry, Royal Institute of Chemistry, S-10044 Stockholm, Sweden
[c] Department of Chemistry, The University of Auckland, Private Bag 92019, Auckland, New Zealand

  1434−1948/99/0404−0633 $ 17.50+.50/0

the synthesis of such mercury species. In addition, the interaction between the mercury species and the solvent, i.e. gallates and arene, is of interest because of the unusual coordination chemistry displayed by the previously investigated metal−metal-bonded bisarene compounds $[Pd_2(AlCl_4)_2](C_6H_6)_2$, $[Pd_2(Al_2Cl_7)_2](C_6H_6)_2$,[29−31] and $[Hg_2(C_9H_{12})_2](AlCl_4)_2$ (C_6H_6 = benzene; C_9H_{12} = mesitylene).[32] In the Pd compounds, the aluminates occupy the primary coordination site along the Pd−Pd bond vector and the benzene molecules sandwich the Pd_2^{2+} core. Surprisingly, the opposite is true for the dimercury compound, where mesitylene occupies the primary coordination site. In the case of mercury, this site is normally occupied by anionic, hard bases with donor atoms such as oxygen, nitrogen, and halogens.[33−35] Nevertheless, the compound $[Hg_2(CO)_2](Sb_2F_{11})_2$ has recently been studied by vibrational spectroscopy and seems to provide another example of linear C−Hg−Hg−C coordination.[36] However, the only isolated, solid compound containing Hg_2^{2+} ions and benzene is $[Hg_2(AlCl_4)_2](C_6H_6)_2$.[37] Unfortunately, this compound has never been completely structurally characterised and thus does not shed any light on the Hg_2^{2+}−benzene interaction and the competition between benzene and chloroaluminate ions for the primary coordination sites of the cation.

The aim of the present work is twofold: firstly, to investigate the stability of subvalent mercury species in aromatic solvents and, secondly, to elucidate the coordination of aromatic molecules by such species.

Experimental Results and Discussion

Throughout this work the abbreviation X°(A;B) will be used to denote the mol fraction of component A with respect to component B in ternary or higher order systems; i.e. $X°(A;B) = n_A/(n_A + n_B)$.

The $Hg_2Cl_2/GaCl_3$/Benzene System

The solubility of Hg_2Cl_2 in a 30 mol-% $GaCl_3$/benzene solution approximately corresponds to $X°(Hg_2Cl_2;GaCl_3) = 0.15$. Solutions saturated with Hg_2Cl_2 consist of two liquid phases in equilibrium with solid Hg_2Cl_2. The less dense, colourless phase constitutes only a minor part of the total volume and Raman and NMR spectra indicate that it essentially consists of pure benzene. The Raman spectrum of the denser, faintly yellow liquid phase is more informative (Figure 1, Table 1) and the bands are readily assigned. The strong band at 154 cm^{-1} coincides with the Hg−Hg stretch frequency of Hg_2Cl_2 in Hg−$HgCl_2$ melts.[38] In addition, the band at 368 cm^{-1} (the symmetrical, terminal $GaCl_3$ stretch in $Ga_nCl_{3n+1}^-$)[25] and the lack of bands belonging to Ga_2Cl_6 unambigously show that $GaCl_3$ acts as a chloride acceptor in the dissolution of Hg_2Cl_2 in $GaCl_3$/benzene solution (Equation 1).

$$Hg_2Cl_2 + 2n\ GaCl_3 \rightarrow Hg_2^{2+} + 2\ Ga_nCl_{3n+1}^- \quad (1)$$

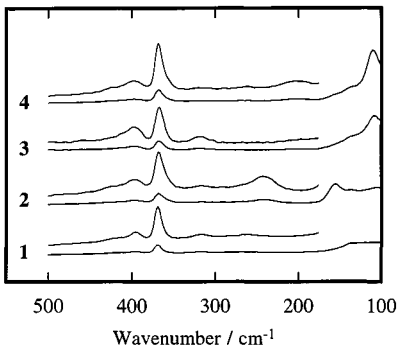

Figure 1. The Raman spectra of (1) the $Ga/GaCl_3/C_6H_6$ system, $X°(Ga;GaCl_3) = 0.191$; (2) the denser liquid phase of the $Hg_2Cl_2/GaCl_3/C_6H_6$ system saturated with Hg_2Cl_2; (3) the $Hg/GaCl_3/C_6H_6$ system saturated with mercury metal; (4) the denser liquid phase of the $Hg/Hg_2Cl_2/GaCl_3/C_6H_6$ system saturated with Hg_2Cl_2 and metallic mercury; $X°(GaCl_3;C_6H_6) = 0.300$ in all systems; the top spectrum of each pair is shown on an expanded scale

The band at 368 cm^{-1} is markedly skew-symmetric relative to the corresponding band observed in $Ga/GaCl_3$/benzene solutions,[25] which suggests a lowering of the local symmetry of the terminal $GaCl_3$ groups in the presence of Hg_2^{2+}. Such a lowering of the $GaCl_3$ symmetry is presumably caused by an interaction between the anions and Hg_2^{2+}. Further inspection of the Raman spectra reveals other indications of strong interactions between Hg_2^{2+} and chlorogallate ions. Thus, the band at 241 cm^{-1} is found near the position of the Ga−Cl−Ga stretch frequency of $Ga_2Cl_7^-$ in $Ga(Ga_2Cl_7)$/benzene solutions (264 cm^{-1}),[25] but the intensity of the 241 cm^{-1} band is much higher relative to that of the symmetrical, terminal $GaCl_3$ stretch vibration. It therefore seems reasonable to assume that this region of the spectrum contains contributions from modes other than the Ga−Cl−Ga stretch. The Hg−Cl stretch vibration (ν_2, Σ_g^+) in Hg_2Cl_2 has been reported at 260 cm^{-1} in $Hg/HgCl_2$ melts and at 279 cm^{-1} in solid Hg_2Cl_2.[38] A shift of the Hg−Cl band towards lower wavenumbers is to be expected when Cl^- is substituted for the more weakly coordinating $Ga_nCl_{3n+1}^-$ ions. It is therefore plausible that the band at 241 cm^{-1} contains contributions also from Hg−Cl modes. Indeed, a distinct Hg−Cl interaction between Hg_2^{2+} and $Ga_nCl_{3n+1}^-$ is expected since Hg_2^{2+} has previously been shown to form Hg−X bonds with weak Lewis bases such as trifluoroacetate and perchlorate.[39][40] However, it has to be remembered that $Ga_nCl_{3n+1}^-$ ions are not the only Lewis bases present in the $Hg_2Cl_2/GaCl_3$/benzene system; the solvent itself, benzene, is a Lewis base and must be accounted for when discussing the coordination of Hg_2^{2+} in this system. Evidence for an interaction between benzene and Hg_2^{2+} are also found in the Raman data. The totally symmetric, ring-breathing mode (of A_{1g} symmetry in the D_{6h} point group) of C_6H_6 at 993 cm^{-1} is split in the spectra of the $Hg_2Cl_2/GaCl_3$/benzene system and a new band is observed at 978 cm^{-1} (Figure 2). This spectral effect could be the result of a symmetry-lowering of C_6H_6 coordinated to Hg_2^{2+} in a $(Hg_2^{2+})(C_6H_6)_k$ complex, but an activation of the most probable candidate, the C−H bending mode of E_{2u} symmetry, is unlikely to produce such a strong Raman

Table 1. Comparison of Raman bands observed in the $Hg_2Cl_2/GaCl_3$/benzene, $Hg/Hg_2Cl_2/GaCl_3$/benzene and $Hg/GaCl_3$/benzene systems with literature data on the molten Hg-$HgCl_2$ system;[38] the intensity and appearance of the bands are indicated by the following abbreviations: s = strong, m = medium, w = weak, v = very, br = broad, sh = shoulder; the assignments for bands of Ga_2Cl_6 and $Ga_nCl_{3n+1}^-$ are based on data from the $Ga/GaCl_3$ system[25][42]

$Hg_2Cl_2/GaCl_3/C_6H_6$	$Hg/Hg_2Cl_2/GaCl_3/C_6H_6$	$Hg/GaCl_3/C_6H_6$	$Hg/HgCl_2$ (melt)	Assignment
ca. 420 sh	ca. 420 sh			$Ga_2Cl_7^-$
		ca. 410 sh		Ga_2Cl_6
395 m	396 m	398 m		$Ga_nCl_{3n+1}^-$
368 s	368 s	367 s		$Ga_nCl_{3n+1}^-$
317 mw		319 m		$Ga_3Cl_{10}^-$
	254 vw			$Ga_2Cl_7^-$
241 m, br	201 m, br		260 vw	Hg−Cl stretch
		ca. 190 sh, br		?
154 vs			154 vs	Hg−Hg, Hg_2X_2
ca. 135 sh	ca. 135 sh	ca. 135 sh		Ga−Cl deform.
	110 vs	109 vs	100 vs	Hg−Hg, Hg_3X_2

band. Instead, the new peak shifted about 15 cm^{-1} to lower wavenumbers is interpreted as arising from the benzene breathing mode of molecules coordinated to the Hg_2^{2+} core, thus reflecting the difference in C−C bonding between coordinated and noncoordinated benzene molecules.

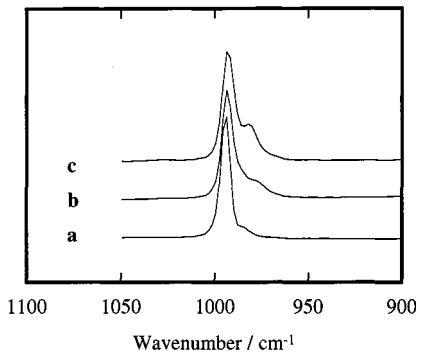

Figure 2. The Raman-spectroscopic effect of Hg_m^{2+} ions on the totally symmetric C_6H_6 ring breathing mode: (a) neat benzene; (b) Hg_2^{2+} in $Hg_2Cl_2/GaCl_3/C_6H_6$ saturated with Hg_2Cl_2; (c) Hg_3^{2+} in $Hg/Hg_2Cl_2/GaCl_3/C_6H_6$ saturated with Hg and Hg_2Cl_2. $X°(GaCl_3;C_6H_6) = 0.300$ in b and c

The IR-active, all-in-phase, out-of-plane C−H bending mode (A_{2u} symmetry) observed at 673 cm^{-1} in benzene, is a sensitive indicator of benzene substitution[41] and, as we will see, coordination. In $GaCl_3$/benzene solution two peaks at 672 and 697 cm^{-1} appear in the IR spectra. The former is identified as the pure benzene A_{2u} band, and the latter is consistent with a shift (+25 cm^{-1}) in frequency of the same vibration mode when benzene is $^1\pi$-coordinated to Ga_2Cl_6.[42] The dissolution of Hg_2Cl_2 in the $GaCl_3$/benzene reaction medium follows Equation 1, where the predominant gallate species formed are $Ga_2Cl_7^-$ and $Ga_3Cl_{10}^-$. In the $Hg_2Cl_2/GaCl_3$/benzene system, we thus expect a strong band at 672 cm^{-1} from noncoordinated benzene, a weak peak at 697 cm^{-1} from benzene coordinated to a small amount of remaining Ga_2Cl_6 and finally a peak from benzene coordinated to Hg_2^{2+}. These expectations are verified and a new band, assigned to benzene in a complex with Hg_2^{2+}, appears at 721 cm^{-1} (shift: +48 cm^{-1} relative to neat benzene).

In ^{13}C-NMR spectra of $Hg_2Cl_2/GaCl_3$/benzene solutions the effects of the inferred complex formation are small and amount to a minor (0.7 ppm in solutions saturated with Hg_2Cl_2) downfield shift of the ^{13}C resonance of C_6H_6 relative to neat benzene. The interaction between aromatic molecules and Hg_2^{2+} has previously been studied by ^{13}C-NMR and Raman spectroscopy in SO_2 solution and a few $(Hg_2^{2+})(arene)_k$ complexes have been isolated from such solution as their hexafluoroarsenate(V) salts.[43][44] No direct structural data were derived, but the results were interpreted in terms of a localized η^2 coordination of C_6H_6 by Hg_2^{2+}. However, the trends in ^{13}C-NMR shifts cannot unambigously be interpreted as coordination effects.

In order to shed further light on the structure of $Hg_2Cl_2/GaCl_3$/benzene solutions, a liquid X-ray scattering investigation (LXS) was performed. Due to the high linear absorptivity of the systems, the data do not allow for a full refinement of a structure model, but the reduced radial distribution function (rRDF, Figure 3) can be evaluated semiquantitatively. The most prominent feature of the rRDF is a strong peak at 2.58 Å which can be assigned to the Hg−Hg correlation. This strong Hg−Hg peak probably overlaps and hides any Hg−Cl or Hg−C correlations. In solid Hg_2Cl_2 the two shortest Hg−Cl distances are found at 2.43 Å,[45] but these can be expected to be somewhat longer for the $Hg_2^{2+}-Ga_nCl_{3n+1}^-$ contacts because of the weaker Lewis basicity of the gallates. The Hg−Hg bond length inferred by the rRDF (2.58 Å) is somewhat longer than in solid Hg_2Cl_2 (2.53 Å)[46] and in aqueous solutions of Hg^I perchlorate (2.52 Å).[47] Unfortunately, the suggested overlap between the Hg−Hg and Hg−Cl (or Hg−C) correlations in the rRDF makes the determination of the Hg−Hg distance uncertain. A detailed interpretation of the inferred bond elongation in terms of coordination effects on Hg_2^{2+} is therefore difficult.

On the basis of the known structural data for the $[Pd_2(AlCl_4)_2](C_6H_6)_2$ and $[Hg_2(C_9H_{12})_2](AlCl_4)_2$ compounds,[29−32] two structural models can be constructed that realistically rationalize the peaks in the rRDF for r values smaller than 5 Å. The two models are depicted schematically in Figures 4a and 4b and are compared with ex-

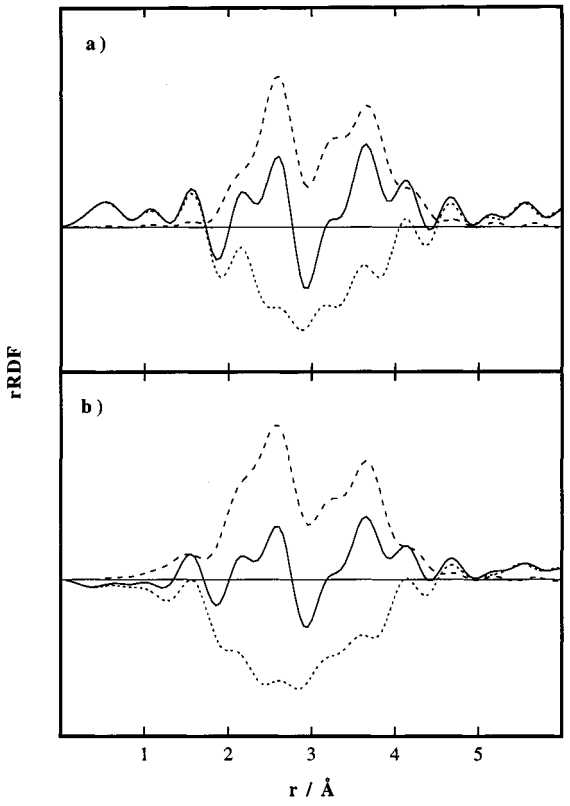

Figure 3. The rRDFs of the $Hg_2Cl_2/GaCl_3/C_6H_6$ (saturated with Hg_2Cl_2) system; X°($GaCl_3$;C_6H_6) = 0.300; the experimental functions are shown as solid lines. The sum of the calculated peak shapes of the two models shown in Figure 4a and 4b are shown as dashed and the difference curves (between experimental data and structural model) as dotted lines in the (a) and (b) figures, respectively

perimental data in the corresponding Figures 3a and 3b. In addition to Hg−Hg and Hg−Cl distances, the models include Ga−Ga, Cl···Cl, terminal Ga−Cl distances, and interaromatic C−C contacts, in agreement with those in benzene solutions of $Ga(Ga_2Cl_7)$.[25] As seen in the Figures 3a and 3b, X-ray scattering alone or in conjunction with spectroscopic data cannot be used to unambigously distinguish between the two structural models. Therefore, we also have to consider the results from quantum-chemical calculations before arriving at a conclusion. These results are reported below, together with those for the Hg_3^{2+} ion.

The $Hg/Hg_2Cl_2/GaCl_3$/Benzene System

The reduction of a $Hg_2Cl_2/GaCl_3$/benzene solution with an excess of metallic mercury yields a dark brown solution. $Hg/Hg_2Cl_2/GaCl_3$/benzene systems saturated with both Hg and Hg_2Cl_2 display two liquid phases, of which the less dense one consists of virtually pure benzene as is evident from its Raman and NMR spectra. The spectral characteristics of the denser liquid phase differ from the corresponding one of the $Hg_2Cl_2/GaCl_3$/benzene solution in several ways:

1. The Hg−Hg Raman band of Hg_2^{2+} at 154 cm^{-1} is replaced by a very strong band at 110 cm^{-1}. This band

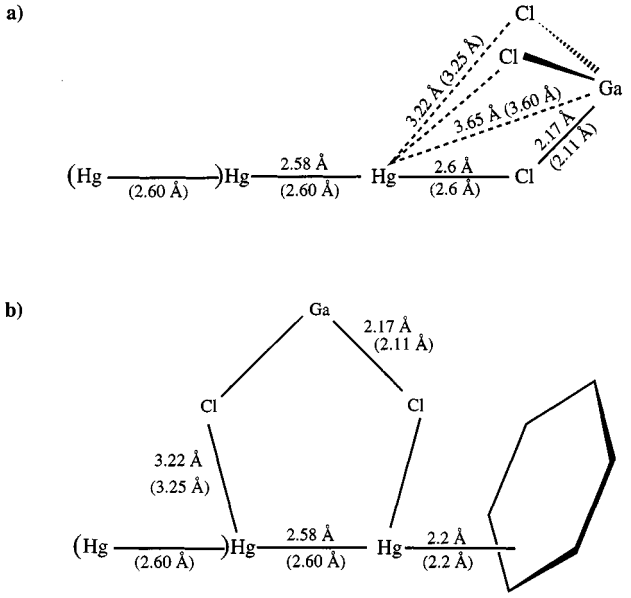

Figure 4. General structural models for (a) the $Hg_m^{2+}-Ga_nCl_{3n+1}^-$ coordination, and (b) the $Hg_m^{2+}-C_6H_6$ coordination compatible with LXS data; distances shown in brackets are those for $m = 3$; those without brackets are for $m = 2$; all distances correspond to peaks in the rRDFs

nearly coincides with that of the Hg_3^{2+} ion in SO_2 solution, reported at 113 cm^{-1}.[2]

2. The band at 241 cm^{-1} is replaced by a less intense band at 201 cm^{-1}. Considering the assignment of this band to Hg−Cl modes, the shift to lower wavenumbers and the decreased intensity suggest a weaker coordination of $Ga_nCl_{3n+1}^-$ to Hg_3^{2+} as compared to Hg_2^{2+}.

3. The ^{199}Hg-NMR resonance at δ = −2103 (relative to $HgMe_2$) observed in $Hg_2Cl_2/GaCl_3$/benzene solutions disappears upon reduction with an excess of metallic Hg. The same NMR-spectroscopic characteristics of Hg_2^{2+} and Hg_3^{2+} have been reported from studies in fluorosulphuric acid and liquid SO_2 solution at room temperature. In these studies, the observation of mercury signals from Hg_3^{2+} was complicated by the enormous Hg−Hg coupling constant and low-temperature experiments were needed to indentify the coupling satellites.[48] Due to the relatively high melting point of benzene, such experiments cannot be performed in this study.

The rRDF of the dense liquid phase from a $GaCl_3$/benzene solution equilibrated with an excess of Hg_2Cl_2 and Hg (Figure 5) is very similar to that of the $Hg_2Cl_2/GaCl_3$/benzene solution at $r < 4$ Å and thus suggests a very similar coordination of the benzene and chlorogallate ions and a nearest neighbour Hg−Hg distance of 2.60 Å. However, a notable feature which is not present in the rRDF of the $Hg_2Cl_2/GaCl_3$/benzene system is the strong peak at 5.15 Å. This value is in good agreement with what should be expected for the correlation between the terminal Hg atoms in a linear Hg_3^{2+} cation with a nearest neighbour Hg−Hg distance of about 2.60 Å. The two alternative general structure models for the rRDF are shown in Figures 4a and 4b, and they are compared with the experimental data in Figures 5a and 5b.

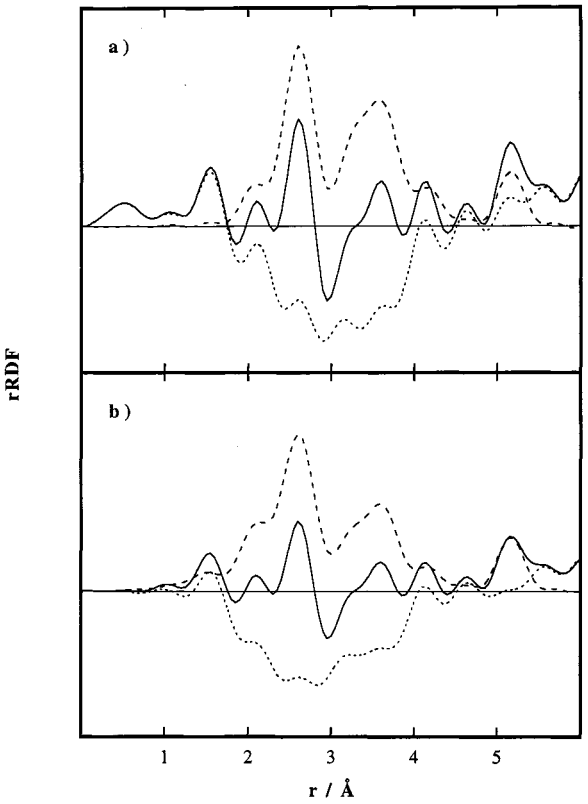

Figure 5. The rRDFs of the $Hg/Hg_2Cl_2/GaCl_3/C_6H_6$ (saturated with Hg and Hg_2Cl_2) systems; $X°(GaCl_3;C_6H_6) = 0.300$; the experimental functions are shown as solid lines; the sum of the calculated peak shapes of the two models shown in Figures 4a and 4b are shown as dashed and the difference curves (between experimental data and structural model) as dotted lines in the (a) and (b) figures, respectively

In the solid state, the Hg_3^{2+} ion has been found to be linear[2] (or very nearly so)[1][5] with Hg−Hg distances ranging between 2.551 and 2.562 Å. The Hg−Hg distance of Hg_3^{2+} in benzene solution (2.60 Å) is thus implied to be somewhat longer than in the solid state and the data therefore parallels the results for the Hg_2^{2+} ion in benzene solution. The $Hg_3^{2+}-C_6H_6$ interaction also seems to parallel that of the Hg_2^{2+} ion. The splitting of the C_6H_6 band at 993 cm^{-1} gives rise to a new band at 982 cm^{-1} in the $Hg/Hg_2Cl_2/GaCl_3$/benzene system (Figure 2), whereas the ^{13}C-NMR resonance in $GaCl_3$/benzene solutions saturated with Hg_2Cl_2 and Hg occurs 0.6 ppm downfield relative to neat benzene. In the IR spectra, the all-in-phase C−H out-of-plane bending mode is shifted to 713 cm^{-1} (shift: +40 cm^{-1}). The spectrum also contains the previously discussed peaks from benzene (673 cm^{-1}) and remaining Ga_2Cl_6−benzene complexes (697 cm^{-1}).

Solubility measurements substantiate the conclusion that Hg_3^{2+} is formed by the oxidation of mercury by Hg_2^{2+}. The solubility measurements were performed in systems where Hg_2Cl_2 was added to transfer essentially all Ga^{III} into $Ga_2Cl_7^-$, according to Equation 1. The only oxidising agent present is thus Hg_2^{2+}, and the solubility was found to be $X°(Hg;Hg_2Cl_2) = 0.958\pm0.005$, thus supporting the interpretation of the spectroscopic data in terms of the reaction $Hg(l) + Hg_2^{2+} \rightarrow Hg_3^{2+}$.

The $Hg/GaCl_3$/Benzene and $Hg/GaCl_3$ Systems − Experimental Evidence for "Soft-Base Stabilisation" of Subvalent Mercury Species

In previous investigations of the reaction between bismuth metal and $GaCl_3$, it transpired that the reactions taking place in $GaCl_3$/benzene solution at room temperature paralleled those in the liquid $GaCl_3$ and $NaCl/GaCl_3$ systems at elevated temperatures.[26][27] In all these solvents, the oxidation of excess bismuth was found to yield concentrated solutions of Bi_5^{3+}, Ga^+, and chlorogallate(III) ions. In stark contrast, the reaction between mercury metal and $GaCl_3$ seems to be thermodynamically dependent on the presence of benzene. Thus, mercury is very soluble in $GaCl_3$/benzene [$X°(Hg;GaCl_3) = 0.226$; $X°(GaCl_3;C_6H_6) = 0.300$], but is insoluble in neat, liquid $GaCl_3$ and only sparingly soluble in liquid $KCl/GaCl_3$ [$X°(Hg;GaCl_3) = 0.024$; $X°(KCl;GaCl_3) = 0.10$]. If an excess of mercury metal is added to a $GaCl_3$/benzene solution, a single, brown liquid phase in equilibrium with mercury metal rapidly is obtained. The Raman spectrum of this solution at low wavenumbers (Figure 1) is very similar to that of the $Hg/Hg_2Cl_2/GaCl_3$/benzene system and confirms the formation of Hg_3^{2+}. In addition, the Raman band at 322 cm^{-1} and the observation of a $^{71}Ga^I$-NMR signal at $\delta = -994$ (relative aqueous $GaCl_4^-$) reveal the concomitant formation of Ga^+ and $Ga_3Cl_{10}^-$ ions, in analogy with the results from $Bi/GaCl_3$/benzene solutions.[26][27] Taken together, these observations strongly suggest Equation 2 to be the predominant reaction between mercury metal and $GaCl_3$ in benzene solution. Assuming a complete reaction between mercury and $GaCl_3$ according to Equation 2, mercury would be soluble to $X°(Hg;GaCl_3) = 0.231$ in the $Hg/GaCl_3$/benzene system. This is in excellent agreement with the experimental value (0.226). In solutions not saturated with Hg metal also Hg_2^{2+} can be synthesised in an analogous manner.

$$3\ Hg + 10\ GaCl_3 \rightarrow Hg_3^{2+} + Ga^+ + 3\ Ga_3Cl_{10}^- \quad (2)$$

It is not feasible to assign the low solubility of mercury metal in liquid $GaCl_3$ and $KCl/GaCl_3$ to a thermal instability of Hg_3^{2+}, since this species has been detected in the chloroaluminate melts at temperatures around 200°C and isolated as tetrachloroaluminate salt from such systems.[1][44] It is therefore tempting to assign the efficient formation of Hg_3^{2+} in $GaCl_3$/benzene solution and the lack of such in liquid $GaCl_3$ and $KCl/GaCl_3$ to stabilising interactions between the arene and the mercury cation. Such interactions, together with those between Ga^+ and benzene, clearly have the potential to push Equation 2 to the right through a formation of $(Hg_3^{2+})(C_6H_6)_k$ complexes and would provide a "base stabilisation" of the subvalent mercury cation. However, Hg_3^{2+} is of course still to be regarded as "acid-stabilised" in the sense that the strongly Lewis-acidic environment ensured by the coordinatively unsaturated $Ga_nCl_{3n+1}^-$ anions prohibits the stabilisation of the Hg^{II} oxidation state through complex formation with chloride and therefore hinders disproportionation. This fact infers a superficially contradictory notion of base stabilis-

ation acting side by side with acid stabilisation. However, the concept of acid stabilisation, as it is normally formulated, is applicable *only* to acid−base equilibria involving hard or intermediate donors and acceptors. This, in turn, is a consequence of the fact that most of the work previously done has involved fluoride and chloride systems. In the present system, the presence of the pronounced *soft* donor C_6H_6 must also be taken into account.

Theoretical Calculations on the Coordination of Hg_m^{2+} Ions

Theoretical calculations were used in an attempt to resolve the experimental ambiguities regarding the coordination of the Hg_m^{2+} ions in $GaCl_3$/benzene media and to substantiate the indications that the subvalent mercury ions are to be regarded as "soft-base-stabilised" in such media. The benzene coordination to the Hg_m^{2+} (m = 2, 3) cores were theoretically investigated in two types of models. In the first type, only interactions between Hg_m^{2+} and two benzene molecules were included; in the second type, also interactions with two chloride ions (as models for gallates/aluminates in the primary coordination site along the Hg−Hg bond vector) were considered. In addition, the separate Hg_m^{2+} and Hg_mCl_2 (m = 2, 3) units where investigated. Models for the coordination of gallates in the secondary site were not considered. The reason is both the ambiguous potential coordination mode and the calculationally huge systems that would emerge.

The quantum-chemical calculations were performed with the GAUSSIAN94 program package.[49] Several potential coordination models for $Hg_m(C_6H_6)_2^{2+}$ and $Hg_mCl_2(C_6H_6)_2$, m = 2 and 3, were optimised at Hartree-Fock level using basis sets of double-zeta quality, viz. LANL2DZ for Hg and 3-21G for the lighter elements. The geometries shown in Figures 6 and 7 represent points of zero gradients on the hypersurface and were identified using the LANL2DZ basis sets (only used for pre-optimisation), later optimised using larger basis sets. The more extended basis sets used for the lighter elements were of augmented 3-21G type; (10s7p)/[5s4p] for Cl, (7s4p)/[4s3p] for C, and (3s)/[2s] for H. The valence space of Hg was optimized at both HF and MP2 level, employing a 60-electron ARECP for Hg,[50] and contracted to (9s9p6d2f)/[6s6p3d1f], where the original f function was omitted because of the lack of gradients for f functions in the combination with ECPs in all common theoretical program packages. Although these basis sets are of moderate size for an atom, the calculations for the molecules were elaborate in computer time and disk space requirements for the full geometry optimisations and frequency calculations, which were performed for all systems at Hartree−Fock (HF) and hybrid density-functional (B3LYP) levels.[51] All systems, except the trimercury ones, were also studied at MP2 level. The HF-optimised basis sets were used for the HF calculations. However, for the correlated calculations the Hg basis set was re-optimised by minimising the MP2 total energy. This has the advantage that basis set superposition errors (BSSE) are suppressed and the bonding involving Hg atoms therefore better described.

The structures in Figure 6 display the $Hg_m(C_6H_6)_2^{2+}$ models in which the chloride ions were not explicitly included and benzene occupies the primary coordination site along the Hg−Hg bond vector. As can be seen from the summary in Tables 2, the energy differences between the η^6, η^2, and η^1/*quasi*-η^3 coordination modes are small but significant. The most stable configuration is the η^1/*quasi*-η^3 one, in good agreement with the crystal structure of $[Hg_2(C_9H_{12})_2](AlCl_4)_2$ (C_9H_{12} = mesitylene).[32] For the $Hg_2(C_6H_6)_2^{2+}$ complex the η^2 mode is 18 kJ mol^{-1} and the η^6 mode 119 kJ mol^{-1} higher in energy (B3LYP level), and the corresponding values for the $Hg_3(C_6H_6)_2^{2+}$ complex are 23 and 99 kJ mol^{-1}. Furthermore, as is obvious from a study of the Hessians, the optimised structures of $Hg_m(\eta^2\text{-}C_6H_6)_2^{2+}$ and $Hg_m(\eta^6\text{-}C_6H_6)_2^{2+}$ (Figure 6) are somewhat too restricted to be considered as proper minima in the strict sense. Negative eigenvalues of the Hessian for these structures correspond to distortions towards the η^1/(*quasi*-η^3) structures. The Hg−Hg bonds are slightly elongated upon coordination to the benzene molecules, and the elongation seems to increase as the hapticity decreases. The charge transfer in the $Hg_m(C_6H_6)_2^{2+}$ complexes is small; the terminal Hg atoms have a formal charge close to +2/m, according to an NBO population analysis. The electron density donation to the terminal Hg atoms seems to be smaller in the trimer than in the dimer, and also the Hg−C distances longer.

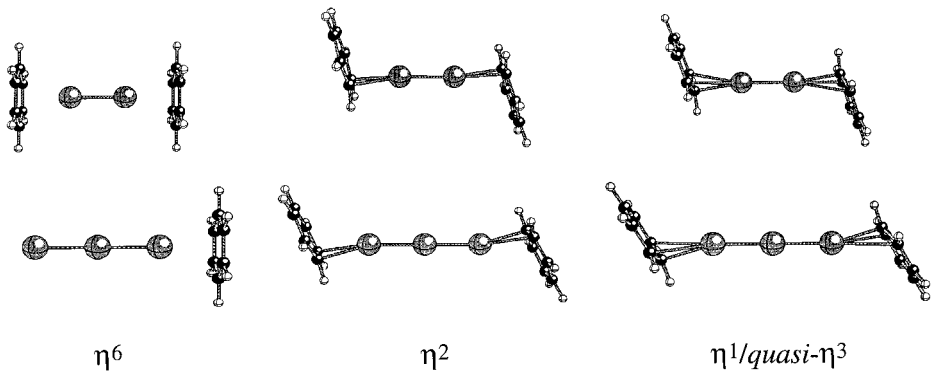

Figure 6. Optimised structures (B3LYP level) of the η^6-, η^2- and η^1/*quasi*-η^3-benzene coordination models for Hg_2^{2+} and Hg_3^{2+}

Table 2. Calulational results including selected atom-atom distances, NLMO/NPA bond orders,[59][60] NBO atom charges[61] and the total energy

System	Method	Distances [Å] Hg−Hg	Hg−Cl	Hg−C	Bond orders Hg−Hg	Hg−Cl	Hg−C	Charges Hg	Cl	bz[a]	Total energy [a.u.]
Hg_2^{2+}											
	HF	2.492			1.00			+1.00			−304.20016
	B3LYP	2.531			1.00			+1.00			−306.15647
	MP2	2.487			1.00			+1.00			−304.56485
Hg_3^{2+}											
	HF	2.495			0.62			+0.67, +0.67[b]			−456.68797
	B3LYP	2.518			0.57			+0.63, +0.68[b]			−459.70361
	MP2	2.477			0.63			+0.64, +0.68[b]			−457.27755
Hg_2Cl_2											
	HF	2.488	2.351		0.83	0.20		+0.87	−0.87		−1219.65913
	B3LYP	2.506	2.357		0.76	0.27		+0.79	−0.79		−1223.09703
	MP2	2.471	2.327		0.80	0.24		+0.81	−0.81		−1220.16356
Hg_3Cl_2											
	HF	2.490	2.376		0.64	0.19		+0.47, +0.71[b]	−0.94		−1372.06080
	B3LYP	2.506	2.380		0.50	0.24		+0.41, +0.66[b]	−0.86		−1376.54366
	MP2	2.470	2.347		0.55	0.22		+0.42, +0.67[b]	−0.88		−1372.78548
bz[a]											
	HF									+0.00	−229.43935
	B3LYP									+0.00	−230.99729
	MP2									+0.00	−229.96685
$Hg_2(bz)_2^{2+}$											
η^6	HF	2.532		2.761	0.91		0.03[c]	+0.99		+0.01	−763.30212
	B3LYP	2.530		2.721	0.88		0.04[c]	+0.94		+0.06	−768.40616
	MP2	2.510		2.661	0.88		0.04[c]	+0.97		+0.03	−764.77296
η^2	HF	2.556		2.452[d]	0.85		0.12[d]	+0.93		+0.07	−763.33120
	B3LYP	2.584		2.438[d]	0.77		0.17[d]	+0.85		+0.15	−768.44496
	MP2	2.538		2.380[d]	0.82		0.09[d]	+0.90		+0.10	−764.80092
η^1	HF	2.571		2.297[e]	0.83		0.17[e]	+0.92		+0.08	−763.33664
	B3LYP	2.599		2.279[e]	0.74		0.23[e]	+0.83		+0.17	−768.45165
	MP2	2.552		2.236[e]	0.79		0.20[e]	+0.88		+0.12	−764.80488
$Hg_3(bz)_2^{2+}$											
η^6	HF	2.523		2.800	0.61		0.03[c]	+0.70, +0.70[b]		−0.05	−915.77249
	B3LYP	2.536		2.761	0.57		0.01[c]	+0.63, +0.69[b]		−0.01	−921.92264
η^2	HF	2.543		2.468[d]	0.65		0.10[d]	+0.65, +0.70[b]		−0.02	−915.79738
	B3LYP	2.557		2.446[d]	0.48		0.12[d]	+0.56, +0.67[b]		+0.05	−921.95179
η^1	HF	2.557		2.299[e]	0.65		0.16[e]	+0.64, +0.71[b]		−0.03	−915.80556
	B3LYP	2.570		2.271[e]	0.48		0.31[e]	+0.55, +0.68[b]		+0.05	−921.96042
$Hg_2Cl_2(bz)_2$											
	HF	2.600	2.459	3.177[d]	0.81	0.11	−0.01[d]	+0.93	−0.84	−0.09	−1678.63180
	B3LYP	2.617	2.461	3.107[d]	0.74	0.15	−0.01[d]	+0.84	−0.75	−0.09	−1685.18161
	MP2	2.582	2.438	3.011[d]	0.77	0.13	−0.01[d]	+0.88	−0.77	−0.11	−1680.21800
$Hg_3Cl_2(bz)_2$											
	HF	2.636	2.465	3.170[f]	0.60	0.10	0.04[f]	+0.62, +0.78[b]	−0.86	−0.23	−1831.12024
	B3LYP	2.636	2.461	3.114[f]	0.50	0.14	−0.05[f]	+0.55, +0.70[b]	−0.77	−0.21	−1838.70274

[a] bz = benzene. − [b] Charge on central Hg atom (first value) and terminal ones (second value). − [c] Average value for all six Hg−C correlations. − [d] Shortest two Hg−C distances and the corresponding average bond order. − [e] Shortest Hg−C distance and the corresponding bond order. − [f] Shortest two Hg−C distances from the central Hg atom and the corresponding average bond order.

In the optimized $Hg_mCl_2(C_6H_6)_2$ models (with chlorides in the primary coordination sites, Figure 7), the electron donation to Hg is substantially larger than in $Hg_m(C_6H_6)_2^{2+}$ (Table 2). Also, the Hg−C bonds are considerably longer, and the benzene coordination is best characterised as η^2 for both $m = 2$ and $m = 3$. In $Hg_2Cl_2(C_6H_6)_2$, the two Hg atoms coordinate in an identical manner, whereas in $Hg_3Cl_2(C_6H_6)_2$ the main benzene coordination is to the central atom of lowest positive charge. In both cases, the coordination mode and distances are very similar to the arene complexes of Pd_2^{2+}, Cu^+, and Ag^+ ions.[29−31,52−54] Inclusion of benzene molecules to the Hg_mCl_2 structures causes a weakening of the Hg−Cl interaction, and a substantial elongation of the Hg−Hg bonds to about 2.6 Å. Furthermore, in $Hg_3Cl_2(C_6H_6)_2$, the charge transfer from benzene to the central Hg atom is substantial, giving the central atom almost the same positive charge as the terminal ones.

According to the calculations, the energy changes for the Equations 3a and 3b are all strongly favourable. At B3LYP level the changes in energy are −789 ($m = 2$) and −688 kJ mol^{-1} ($m = 3$) for Equation 3a, and −236 ($m = 2$) and −432 kJ mol^{-1} ($m = 3$) for Equation 3b.

$$Hg_m^{2+} + 2\ C_6H_6 \rightarrow Hg_m(\eta^1\text{-}C_6H_6)_2^{2+} \quad (3a)$$

$$Hg_mCl_2 + 2\ C_6H_6 \rightarrow Hg_mCl_2(\eta^2\text{-}C_6H_6)_2 \quad (3b)$$

From the calculations, a few general trends regarding the benzene coordination can be discerned: The coordination of benzene to Hg_2^{2+} is more favourable than to Hg_3^{2+}, but this trend is reversed for Hg_mCl_2 (with chlorides in the primary coordination sites). As indicated by the Hg−C bond

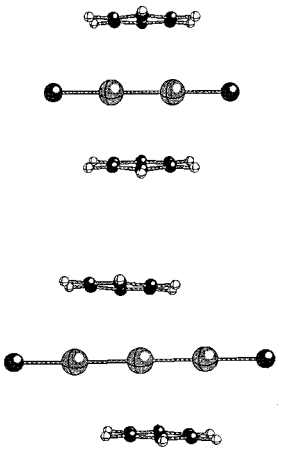

Figure 7. Optimised structures (B3LYP level) of the benzene/gallate coordination models for Hg_2^{2+} and Hg_3^{2+}

lengths, the interaction seems to be energetically stronger between the Hg_m^{2+} ions and benzene, than between the Hg_mCl_2 units and benzene. However, this is a highly simplified analysis, totally disregarding the difference in direct gallate/aluminate−mercury interaction.

Conclusions Based on the Conjunction of Experimental and Theoretical Results

The LAXS data for the Hg_m^{2+} cores in $GaCl_3$/benzene media indicate an elongation of the Hg−Hg distance in such media relative to that in the solid state and molten-salt systems. This evidence finds support in the theoretical calculations, in so far as the calculations suggest that the coordination of benzene to both Hg_m^{2+} and Hg_mCl_2 increase the Hg−Hg distance by a magnitude in good agreement with the experimental results. The calculated Hg−Hg stretch frequencies of the model compounds $Hg_mCl_2(\eta^2\text{-}C_6H_6)_2$ are close to those observed experimentally (Table 3). This is also true for the $Hg_m(C_6H_6)_2^{2+}$ models, irrespective of hapticity, and the influence of benzene coordination on the Hg−Hg stretch frequency thus cannot be used to elucidate the preferred coordination of benzene and chloride by the Hg_m cores.

According to the calculations, the inclusion of benzene molecules to the Hg_mCl_2 structures causes a weakening of the Hg−Cl interaction, consistent with the experimentally observed shift of the Hg−Cl stretch frequencies in benzene media as compared with Hg_mCl_2 melts. The calculated Hg−Cl stretch frequencies (Table 3) are slightly too high at all levels relative to the experimental ones, indicating that the current level of approximation overbind the Hg−Cl interaction. This is expected and unavoidable in the present models, since $Ga_nCl_{3n+1}^-$ ions are weaker Lewis bases than chlorides.

The LAXS and NMR data cannot distinguish between the benzene coordination modes in Figures 6 and 7, although the lack of distinct Hg−C correlations in the rRDFs can be taken as a primitive indication for a low hapticity of the benzene coordination. Nevertheless, the relatively small energy differences between the different coordination modes may indicate a fluxional behavior in solution, consistent with the lack of detailed NMR-spectroscopic data for the benzene interaction. A frontier orbital analysis is consistent with the experimentally observed shift in frequency of the benzene ring breathing mode to lower wavenumbers, assuming an electron-density donation from the bonding benzene π system to the s-dominated, Hg−Hg-antibonding LUMO of the Hg_m^{2+} units. However, of most interest are the calculated shifts in C−C breathing and C−H all-in-phase, out-of-plane mode frequencies of the coordinated benzene molecules for the eight structure models in Figures 6 and 7 (Table 3). It seems clear from the calculations that *only* the end-on coordination of benzene (Figure 6) produces a shift in the C−C mode of a magnitude comparable to the experimental values. The strong and clear effect for the benzene ring breathing mode is a rather convincing evidence for a benzene coordination in the Hg−Hg direction. Also the shift in C−H bending frequencies is best in agreement with the experimental results for the $Hg_m(C_6H_6)_2^{2+}$ models. However, the calculations suggest that the energy of two monomeric $Hg(\eta^2\text{-}C_6H_6)^+$ complexes has about the same energy as $Hg_2(\eta^2\text{-}C_6H_6)_2^{2+}$ at both HF and B3LYP level (Table 2). This indicates that the benzene-coordinated dimer requires the extra stabilisation provided by gallates in the secondary (sandwiching) coordination site. Consequently, it seems that both the presence of benzene *and* gallate anions are important for the stabilisation of subvalent mercury species in benzene solution. This is in good agreement with our experimental data, which are consistent with a strong interaction between both the anionic, hard gallates and the neutral, soft benzene molecules, of which the latter clearly is a fundamental prerequisite for the formation of subvalent mercury ions in the Hg/$GaCl_3$/benzene system.

To conclude, both coordination models proposed for Hg_2^{2+} and Hg_3^{2+} are theoretically feasible, and the current systems are thus highly interesting in terms of the competition between hard and soft donor ligands for the primary coordination site. However, in view of the experimental and quantum-chemical results we are inclined to favour the coordination model with η^1/*quasi*-η^3-benzene along the Hg−Hg bond vector and the gallates confined to a secondary coordination site (Figure 6). The possible "base stabilisation" of subvalent clusters by aromatics definitely deserves further experimental and theoretical investigation since interactions with hetero groups (carbonyl transition metal compounds) recently have been shown to be a way to stabilise new and unprecedented clusters of the post-transition elements.[55−58] However, results derived for the subvalent Hg_m^{2+} ions must be applied with considerable care on other subvalent post-transition element clusters, since the mercury species are unique in their strong interaction with the counterions.

Experimental Section

General: All sample preparations were performed in a glove box under dried, deoxygenated nitrogen (< 1 ppm H_2O). All glassware

Table 3. Calulated vibrational frequencies for the Hg−Hg, Hg−Cl, and important internal benzene modes

System	Method	Hg−Hg stretch [cm^{-1}] symm	Hg−Hg stretch [cm^{-1}] asymm	Hg−Cl stretch [cm^{-1}] symm	Hg−Cl stretch [cm^{-1}] asymm	C−C breathing[a] [cm^{-1}] average	C−C breathing[a] [cm^{-1}] Δ[c]	C−H bending[b] [cm^{-1}] average	C−H bending[b] [cm^{-1}] Δ[c]
Hg_2^{2+}									
($D_{\infty h}$)	HF	222(Σ_g^+)							
	B3LYP	193(Σ_g^+)							
	MP2	216(Σ_g^+)							
Hg_3^{2+}									
($D_{\infty h}$)	HF	158(Σ_g^+)	273(Σ_u^+)						
	B3LYP	142(Σ_g^+)	252(Σ_u^+)						
	MP2	158(Σ_g^+)	276(Σ_u^+)						
Hg_2Cl_2									
($D_{\infty h}$)	HF	203(Σ_g^+)		379(Σ_g^+)	352(Σ_u^+)				
	B3LYP	186(Σ_g^+)		372(Σ_g^+)	347(Σ_u^+)				
	MP2	205(Σ_g^+)		394(Σ_g^+)	367(Σ_u^+)				
Hg_3Cl_2									
($D_{\infty h}$)	HF	148(Σ_g^+)	261(Σ_u^+)	350(Σ_g^+)	350(Σ_u^+)				
	B3LYP	136(Σ_g^+)	248(Σ_u^+)	349(Σ_g^+)	346(Σ_u^+)				
	MP2	150(Σ_g^+)	268(Σ_u^+)	367(Σ_g^+)	366(Σ_u^+)				
bz[d]									
(D_{6h})	HF					1067(A_{1g})		794(A_{2u})	
	B3LYP					1006(A_{1g})		708(A_{2u})	
	MP2					980(A_{1g})		686(A_{2u})	
	exp					993(A_{1g})		673(A_{2u})	
$Hg_2(bz)_2^{2+}$									
(D_{6h}), η^6	HF	134(A_{1g})				1044(A_{1g},A_{2u})	−23	840(A_{1g},A_{2u})	+46
	B3LYP	133(A_{1g})				999(A_{1g},A_{2u})	−7	755(A_{1g},A_{2u})	+48
	MP2	140(A_{1g})				955(A_{1g},A_{2u})	−25	744(A_{1g},A_{2u})	+58
(C_{2h}), η^2	HF	183(A_g)				1038(A_g,B_u)	−29	865(A_g,B_u)	+71
	B3LYP	167(A_g)				983(A_g,B_u)	−23	779(A_g,B_u)	+71
	MP2	180(A_g)				951(A_g,B_u)	−29	762(A_g,B_u)	+76
(C_{2h}), η^1	HF	177(A_g)				1025(A_g,B_u)	−42	869(A_g,B_u)	+75
	B3LYP	160(A_g)				961(A_g,B_u)	−45	783(A_g,B_u)	+75
	MP2	182(A_g)				955(A_g,B_u)	−25	745(A_g,B_u)	+59
$Hg_3(bz)_2^{2+}$									
(D_{6h}), η^6	HF	109(A_{1g})	262(A_{2u})			1050(A_{1g},A_{2u})	−17	818(A_{1g},A_{2u})	+24
	B3LYP	105(A_{1g})	252(A_{2u})			987(A_{1g},A_{2u})	−19	739(A_{1g},A_{2u})	+31
(C_{2h}), η^2	HF	144(A_g)	226(B_u)			1049(A_g,B_u)	−11	861(A_g,B_u)	+67
	B3LYP	135(A_g)	218(B_u)			986(A_g,B_u)	−20	772(A_g,B_u)	+64
(C_{2h}), η^1	HF	137(A_g)	222(B_u)			1046(A_g,B_u)	−21	861(A_g,B_u)	+67
	B3LYP	127(A_g)	212(B_u)			977(A_g,B_u)	−29	772(A_g,B_u)	+64
$Hg_2Cl_2(bz)_2$									
(D_{2h})	HF	157(A_1)		313(A_1)	287(A_1)	1064(A_1,B_2)	−3	821(A_1,B_2)	+27
	B3LYP	146(A_1)		306(A_1)	284(A_1)	1002(A_1,B_2)	−4	740(A_1,B_2)	+32
$Hg_3Cl_2(bz)_2$									
(C_{2h})	HF	104(A_g)	186(B_u)	302(A_g)	295(B_u)	1065(A_g,B_u)	−2	824(A_g,B_u)	+30
	B3LYP	99(A_g)	182(B_u)	301(A_g)	295(B_u)	1003(A_g,B_u)	−3	739(A_g,B_u)	+31

[a] The average benzene ring breathing mode (ν_2). In the mercury compounds, the two benzene rings can vibrate in and out of phase, thus giving rise to two modes with frequencies that normally only differ by a few wavenumbers. Formally, only the A-symmetry mode is Raman-active, but in order to minimise the effect of extensive mixing with other modes in the lower symmetries the average of the two are used. − [b] The all-in-phase C−H bending mode perpendicular to the benzene plane, normally sensitive to ring substitution and coordination. In the mercury complexes, the H atoms in the two benzene rings can vibrate in and out of phase, giving rise to two bands with very similar frequencies. − [c] The difference with respect to the corresponding calculated frequency for free benzene. − [d] bz=benzene.

was dried at 300°C in vacuo prior to use. After sample preparation all sample cells were sealed under vacuum. Hg_2Cl_2 (Merck, p.A. grade) was dried at 150°C for several weeks prior to use. Benzene was distilled and stored over sodium. $GaCl_3$ (ALFA, 99.999%) and mercury metal (Merck, p.A. grade) were used as received. KCl (Merck. p.A.) was dried for several days at 130°C before use. The solubility measurements were made gravimetrically, monitoring the amount of dissolved mercury metal at equilibrium with known amounts of Hg_2Cl_2, $GaCl_3$, and benzene.

Liquid X-ray Scattering (LXS): The LXS experiments were performed at room temperature using Mo-K_α radiation and a Seifert GSD θ−θ diffractometer equipped with a liquid-nitrogen-cooled solid-state detector (Ortec EG&G). The samples were enclosed in sealed Lindemann capillaries with an outer diameter of 1 mm. The experimental procedure and data evaluation have previously been described in detail.[62] The nominal composition of the solvent was $X°(GaCl_3;C_6H_6)$ = 0.29 and the samples were saturated with Hg_2Cl_2 or Hg/Hg_2Cl_2 in order to maximise the contributions from mercury species to the intensity function $s{\cdot}i(s)$ ($s = 4\pi\sin\theta/\lambda$). Data were collected in the s range 0.200−13.00 $Å^{-1}$. In the data evaluation, corrections for spurious peaks in the reduced radial distribution function were applied for $r < 1.0$ Å and the value of k in the damping function $\exp(-ks^2)$ was set to 0.012.

Vibrational Spectroscopy: Raman spectra were recorded with a Bruker IFS-66/FRA-106 FT Raman spectrometer equipped with a low-power Nd:YAG laser (λ = 1064 nm) and a liquid-nitrogen-cooled, solid-state Ge diode detector. The samples were contained in 5-mm NMR tubes sealed under vacuum. The IR spectra were recorded with a Bio-Rad FTS 6000 FT-IR spectrometer, using a Globular radiation source and KBr beamsplitter and DTGS detector, and 6.25 μm Mylar beamsplitter and PE-DTGS detector for the mid-IR and far-IR spectra, respectively. The resolution in both

Raman and IR spectra was 4 cm^{-1}. The samples were prepared in a glove box (vide supra) and contained in polyethylene bags in the far-IR and between Teflon-coated KBr pellets in mid-IR experiments.

NMR Spectroscopy: The NMR measurements were performed with a Varian Unity 300-MHz spectrometer. TMS was used as a reference for the ^{13}C-NMR spectra, whereas ^{199}Hg- and ^{71}Ga-NMR shifts were determined relative to $HgMe_2$ and $GaCl_4^-$ in hydrochloric acid, respectively.

Acknowledgments

This work has been supported by the Swedish Natural Science Research Council and the Human Capital and Mobility (contract no. CHRX CT93 0277). The PDC at the Royal Institute of Technology in Stockholm and the NSC at Linköping University are acknowledged for their allocation of computer resources. P. S. thanks the Marsden Fund (Wellington) for financial support.

[1] R. D. Ellison, H. A. Levy, K. W. Fung, *Inorg. Chem.* **1972**, *11*, 833−836.
[2] B. D. Cutforth, C. G. Davies, P. A. W. Dean, P. R. Ireland, P. K. Ummat, *Inorg. Chem.* **1973**, *12*, 1343−1347.
[3] B. D. Cutforth, R. J. Gillespie, P. R. Ireland, *J. Chem. Soc., Chem. Comm.* **1973**, 723−724.
[4] B. D. Cutforth, R. J. Gillespie, P. R. Ireland, J. F. Sawyer, P. K. Ummat, *Inorg. Chem.* **1983**, *22*, 1344−1347.
[5] I. D. Brown, R. J. Gillespie, K. R. Morgan, J. F. Sawyer, K. J. Schmidt, Z. Tun, P. K. Ummat, J. E. Vekris, *Inorg. Chem.* **1987**, *26*, 689−693.
[6] P. Ganal, P. Moreau, G. Ouvrard, M. Sidorov, M. McKelvy, W. Glaunsinger, *Chem. Mater.* **1995**, *7*, 1132−1139.
[7] M. Sidorov, M. McKelvy, R. Sharma, W. Glaunsinger, P. Ganal, P. Moreau, G. Ouvrard, *Chem. Mater.* **1995**, *7*, 1140−1145.
[8] A. J. Schulz, J. M. Williams, N. D. Miro, A. G. MacDiarmid, A. J. A. Heeger, *Inorg. Chem.* **1978**, *17*, 646−649.
[9] I. D. Brown, B. D. Cutforth, C. G. Davies, R. J. Gillespie, P. R. Ireland, J. E. Vekris, *Can. J. Chem.* **1974**, *52*, 791−793.
[10] N. D. Miro, A. G. MacDiarmid, A. J. Heeger, A. F. Garito, C. K. Chiang, A. J. Schultz, J. M. Williams, *J. Inorg. Nucl. Chem.* **1978**, *40*, 1351−1355.
[11] Z. Tun, I. D. Brown, *Acta Crystallogr., Sect. B* **1982**, *38*, 2321−2324.
[12] Z. Tun, I. D. Brown, P. K. Ummat, *Acta Crystallogr., Sect. C* **1984**, *40*, 1301−1303.
[13] W. R. Datars, P. K. Ummat, R. J. Gillespie, *Mater. Res. Bull.* **1985**, *20*, 865−869.
[14] E. Batalla, W. R. Datars, D. Chartier, R. J. Gillespie, *Solid State Commun.* **1981**, *38*, 1203−1205.
[15] I. J. Dinser, W. R. Datars, D. Chartier, R. J. Gillespie, *Solid State Commun.* **1979**, *32*, 1041−1043.
[16] W. R. Datars, A. van Schyndel, J. S. Lass, D. Chartier, R. J. Gillespie, *Phys. Rev. Lett.* **1978**, *40*, 1184−1187.
[17] E. Batalla, W. R. Datars, D. Chartier, R. J. Gillespie, *Solid State Commun.* **1981**, *40*, 711−714.
[18] D. Chartier, W. R. Datars, R. J. Gillespie, *Can. J. Phys.* **1983**, *61*, 71−75.
[19] F. S. Razavi, W. R. Datars, D. Chartier, R. J. Gillespie, *Phys. Rev. Lett.* **1979**, *42*, 1182−1185.
[20] H. Kunkely, A. Vogler, *Chem. Phys. Lett.* **1995**, *240*, 31−34.
[21] J. D. Corbett, *Prog. Inorg. Chem.* **1976**, *21*, 129−159.
[22] A. Mühlecker-Knoepfler, E. Ellmerer-Müller,R. Konrat, K.-H. Ongania, K. Wurst, P. Peringer, *J. Chem. Soc., Dalton Trans.* **1997**, 1607−1610.
[23] W. R. Mason, *Inorg. Chem.* **1997**, *36*, 1164−1167.
[24] A. Knoepfler, K. Wurst, P. Peringer, *J. Chem. Soc., Chem. Commun.* **1995**, 131−132.
[25] S. Ulvenlund, A. Wheatley, L. A. Bengtsson, *J. Chem. Soc., Dalton Trans.* **1995**, 245−254.
[26] S. Ulvenlund, A. Wheatley, L. A. Bengtsson, *J. Chem. Soc., Chem.* Commun. **1995**, 59−60.
[27] S. Ulvenlund, K. Ståhl, L. Bengtsson-Kloo, *J. Chem. Soc., Faraday Trans.* **1995**, *91*, 4223−4233.
[28] S. Ulvenlund, K. Ståhl, L. Bengtsson-Kloo, *Inorg. Chem.* **1996**, *35*, 223- 230.
[29] G. Allegra, A. Immirzi, L. Porri, *J. Am. Chem. Soc.* **1965**, *87*, 1394−1395.
[30] G. Allegra, G. Tettamanti Casagranda, A. Immirtzi, L. Porri, G. Vitulli, *J. Am. Chem. Soc.* **1970**, *92*, 289−293.
[31] G. Nardin, P. Delise, G. Allegra, *Gazz. Chim. Ital.* **1975**, *105*, 1047−1053.
[32] W. Frank, B. Dincher, *Z. Naturforsch., B* **1987**, *42*, 828−834.
[33] M. Taylor, in *Metal-to-Metal Bonded States of the Main-Group Elements*, Academic Press, New York, **1975**, ch. 2, p. 20−24.
[34] A. F. Wells, *Structural Inorganic Chemistry*, 5th ed., Clarendon Press, Oxford, **1984**, p. 1157−1158.
[35] *Inorganic Reactions and Methods*, vol. 13 (Ed.: A. P. Hagen), VCH, Weinheim, **1991**, p. 363−374.
[36] M. Bodenbinder, G. Balzer-Jöllenbeck, H. Willner, R. J. Batchelor, F. W. B. Einstein, C. Wang, F. Aubke, *Inorg. Chem.* **1996**, *35*, 82−92.
[37] R. W. Turner, E. L. Amma, *J. Inorg. Nucl. Chem.* **1966**, *28*, 2411−2413.
[38] G. A. Voyiatzis, G. N. Papatheodorou, *Inorg. Chem.* **1992**, *31*, 1945- 1951.
[39] M. Sikirica, D. Grdenic, *Acta Crystallogr., Sect. B* **1974**, *30*, 144−146.
[40] G. Johansson, *Acta Chem. Scand.* **1966**, *20*, 553−562.
[41] G. Herzberg, in *Molecular Spectra and Molecular Structure*, Krieger Publishing Co., Malabar, **1991**, vol. II, p. 362−369.
[42] L. Bengtsson-Kloo, S. Ulvenlund, *Spectrochim. Acta, Part A* **1997**, *53*, 2129−2138.
[43] P. A. W. Dean, D. G. Ibbott, J. B. Stothers, *J. Chem. Soc., Chem. Commun.* **1973**, 626−627.
[44] P. A. W. Dean, D. G. Ibbott, J. B. Stothers, *Can. J. Chem.* **1976**, *54*, 166- 176.
[45] E. Dorm, *J. Chem. Soc., Chem. Commun.* **1971**, 466−467.
[46] A. Haaland, *Angew. Chem.* **1989**, *101*, 1017−1032; *Angew. Chem. Int. Ed. Engl.* **1989**, *28*, 992−1007.
[47] E. Biehl, H. J. Deiseroth, *Z. Kristallogr.* **1996**, *211*, 630.
[48] R. J. Gillespie, P. Granger, K. R. Morgan, G. J. Schrobilgen, *Inorg.* Chem. **1984**, *23*, 887−891.
[49] M. J. Frisch, G. W. Trucks, H. B. Schlegel, P. M. W. Gill, B. G. Johnson, M. A. Robb, J. R. Cheeseman, T. A. Keith, G. A. Petersson, J. A. Montgomery, K. Raghavshari, M. A. Al-Laham, V. G. Zakrzewski, J. V. Ortiz, J. B. Foresman, J. Cioslowski, B. B. Stefanov, A. Nanayakkara, M. Challacombe, C. Y. Peng, P. Y. Ayala, W. Chen, M. W. Wong, J. L. Andres, E. S. Replogle, R. Gomperts, R. L. Martin, D. J. Fox, J. S. Binkley, D. J. Defrees, J. Baker, J. P. Stewart, M. Head-Gordon, C. Gonzalez, J. A. Pople, GAUSSIAN94, Gaussian Inc., Pittsburgh PA, **1995**.
[50] U. Häussermann, M. Dolg, H. Stoll, H. Preuss, P. Schwerdtfeger, R. M. Pitzer, *Molec. Phys.* **1993**, *78*, 1211−1224.
[51] A. D. Becke, *J. Chem. Phys.* **1993**, *98*, 5648−5652.
[52] R. W. Turner, E. L. Amma, *J. Am. Chem. Soc.* **1966**, *88*, 1877−1882.
[53] H. G. Smith, R. E. Rundle, *J. Am. Chem. Soc.* **1958**, *80*, 5075−5080.
[54] E. A. H. Griffith, E. L. Amma, *J. Am. Chem. Soc.* **1971**, *93*, 3167−3172.
[55] S. Charles, B. W. Eichhorn, A. L. Rheingold, S. G. Bott, *J. Am. Chem.* Soc. **1994**, *116*, 8077−8086.
[56] A. Seigneurin, T. Makani, D. J. Jones, J. Roziére, *J. Chem. Soc., Dalton Trans.* **1987**, 2111−2116.
[57] B. Schiementz, G. Huttner, *Angew. Chem.* **1993**, *105*, 295−296; *Angew. Chem. Int. Ed. Engl.* **1993**, *32*, 297−298.
[58] B. W. E. Eichhorn, R. C. Haushalter, *J. Chem. Soc., Chem. Commun.* **1990**, 937−938.
[59] A. E. Reed, F. Weinhold, *J. Chem. Phys.* **1985**, *83*, 1736−1740.
[60] A. E. Reed, P. von Rague Schleyer, *J. Am. Chem. Soc.* **1990**, *112*, 1434−1445.
[61] E. D. Glenning, A. E. Reed, J. E. Carpenter, *Gaussian94*, NBO version 3.1.
[62] S. Ulvenlund, L. A. Bengtsson, L.A. *J. Mol. Struct.* **1994**, *326*, 181−191.

Received November 11, 1998
[I98390]